Local disorder and optical properties in V-shaped quantum wires: Toward one-dimensional exciton systems

T. Guillet,* R. Grousson, and V. Voliotis†
Groupe de Physique des Solides, CNRS, Universités Pierre et Marie Curie et Denis Diderot, 2 place Jussieu, F-75251 Paris Cedex 05, France

X. L. Wang‡ and M. Ogura
Photonics Research Institute, National Institute of Advanced Industrial Science and Technology (AIST), Tsukuba Central 2, Tsukuba 305-8568, Japan
and CREST, Japan Science and Technology Corporation (JST), 4-1-8 Honcho, Kawaguchi 332-0012, Japan
(Received 11 November 2002; revised manuscript received 14 April 3; published 30 July 2003)

The exciton localization is studied in GaAs/GaAlAs V-shaped quantum wires (QWR's) by high spatial resolution spectroscopy. Scanning optical imaging of different generations of samples shows that the localization length has been enhanced as the growth techniques were improved. In the best samples, excitons are delocalized in islands of length of the order of 1 μm, and form a continuum of one-dimensional states in each of them, as evidenced by the $\sqrt{T}$ dependence of the radiative lifetime. On the opposite, in the previous generation of QWR's, the localization length is typically 50 nm and the QWR behaves as a collection of quantum boxes. These localization properties are compared to structural properties and related to the progresses of the growth techniques. The presence of residual disorder is evidenced in the best samples and explained by the separation of electrons and holes due to the large built-in piezoelectric field present in the structure.

DOI: 10.1103/PhysRevB.68.045319 PACS number(s): 78.55.Cr, 78.66.Fd, 71.35.−y

I. INTRODUCTION

The local disorder in semiconductor heterostructures is crucial for the understanding of their physical properties. It leads on a macroscopic point of view to two well-known features in optical spectra: the inhomogeneous broadening of the transitions due to the size and/or composition fluctuations, and the Stokes shift between photoluminescence and absorption spectra which is a signature of localization. The major role of monolayer fluctuations of the heterointerfaces has first been identified in quantum wells (QW's),[1,2] and is even more important in quantum wires (QWR's) due to the increased number of interfaces involved in the electronic confinement. The study of the local optical properties by high spatial resolution spectroscopy, in far-field[3] or in near-field,[4,5] allowed a better insight into the understanding of localization in these structures.

In the best QWR structures grown up to now it has been shown that the random potential felt by the excitons and induced by the structural disorder[6] completely localizes the excitons: the localization length is small and each minimum of the potential behaves as a ''natural'' quantum box,[7] so that the optical properties of the QWR can be interpreted as those of a zero-dimensional (0D) system.[8,9] The specific characteristics of a one-dimensional (1D) system, especially its singular density of states, are therefore blurred out by the disorder. Until now delocalized excitons could only be observed at some given positions of QWR samples as their structural properties were improved,[5] opening the way to the achievement of actual 1D systems.

In this paper we investigate the localization properties of the recent generation of QWR's and compare them to previous samples. The disorder is first studied by our scanning optical imaging spectroscopy technique. In particular the localization length is measured (Sec. II). Its mean value is shown to be ten times larger than in the previous samples, and is much larger than the thermal de Broglie wavelength of the excitons (Sec. III). These new QWR's can therefore be considered as actual 1D systems even on a microscopic point of view. This interpretation is supported by the study of the radiative lifetime as a function of temperature, which is highly dependent on the dimensionality of the local density of states in the structure (Sec. IV). Finally the delocalized excitons are shown to be more sensitive to the presence of a residual disorder in the structure (Sec. V).

The nanostructures studied experimentally are undoped 5-nm-thick $GaAs/Ga_{0.57}Al_{0.43}As$ V-shaped QWR's. They are grown on 4-μm pitched V grooves formed on (001) $\pm 0.1°$ GaAs substrates by flow rate modulation epitaxy which is a modified metal organic vapor phase epitaxy technique.[10,11] Their main features are a very strong lateral confinement leading to energy separation between subbands up to 60 meV, and a large optical anisotropy, characteristic of the valence-band mixing in 1D structures.[12]

II. IMAGING THE DISORDER IN A QUANTUM WIRE

In order to understand exciton localization and its influence on the spectroscopy and the dynamics of QW's or QWR's, we have to model and somehow measure the localization potential felt by the excitons. It is characterized by two main quantities: its amplitude V_{loc} and its typical correlation length L_{loc}. V_{loc} can be related to macroscopic properties like the Stokes shift or the half width of the photoluminescence spectrum, under some assumptions on the shape

of the potential.[2] Its value of 7–10 meV is quite independent of the sample since it simply reflects the change of the confinement energy associated to monolayer fluctuations on the heterointerfaces. On the contrary, the correlation length L_{loc} is closely related to the roughness of the interfaces and depends much more on the growth conditions. This parameter can only be evaluated through microscopic studies which give access to the spatial extension of the excitonic states.

We recently developed an imaging technique in order to study the localization effects in quantum wires. This is an evolution of the microphotoluminescence (μ-PL) experiment, that we called scanning optical imaging spectroscopy. It is the equivalent in far field to the scanning near-field optical microscopy (SNOM). The sample is fixed on the cold finger of a helium cryostat and cooled at 10 K. The laser beam is focused on the sample by a microscope objective with a large numerical aperture (0.6) and the laser spot diameter of 1 μm is diffraction limited. The luminescence is analyzed through an imaging spectrometer coupled to a liquid-nitrogen-cooled charge-coupled device (CCD) detector, and the spectral resolution is 50 μeV. The excitation at 1.77 eV creates carriers in the higher-order bands of the wire and not in the barriers. As the wires are separated by 4 μm, only one single wire is excited over 1 μm in our experiment. The excitation spot can be translated with respect to the sample by moving the microscope objective with piezoelectric actuators with a precision better than 200 nm. At each position the μ-PL spectrum is recorded. We obtain in this way a high-resolution image along the wire axis as well as a high resolution spectrum of a single QWR.

Figure 1 presents two such scanning images obtained on two different generations of quantum wires—denoted previous and new generations hereafter—and two corresponding μ-PL spectra extracted from the images. The sample of the previous generation studied in this work has already been the subject of μ-PL studies,[8] whereas the new generation is much more recent.[13] As it has been well known for a few years,[3] the emission spectrum is not uniform as the excitation spot scans the wire, which means that the excitons are not delocalized over the whole wire. Each bright spot corresponds to a local potential minimum along the wire axis where excitons are trapped. Each peak has been attributed to the emission of the lowest-lying level in such a minimum. Two main differences can be distinguished between the two generations of QWR's: (i) The spectra associated to each localization sites are different: the peaks are very sharp for the previous generation, and their linewidth could not be resolved within our experimental resolution, whereas they are 1 meV broad in the case of the new generation. (ii) The linear density of sites, estimated by counting the spots on the images, is of the order of 10 μm^{-1} for the previous generation of QWR's, and 1 μm^{-1} for the new one. We can therefore roughly estimate the extension of the sites to 100 nm for the previous generation, which is compatible with the value obtained from μ-PL excitation spectra,[8] and to 1 μm for the new generation. Moreover, some emitting sites are extended over distances larger than the spatial resolution of the microscope in the new samples, the spot at $x=15$ μm being, for example, 3 μm long in Fig. 1(c). Most of the emitting sites could, however, not be resolved spatially because their extension is close to or smaller than the resolution.

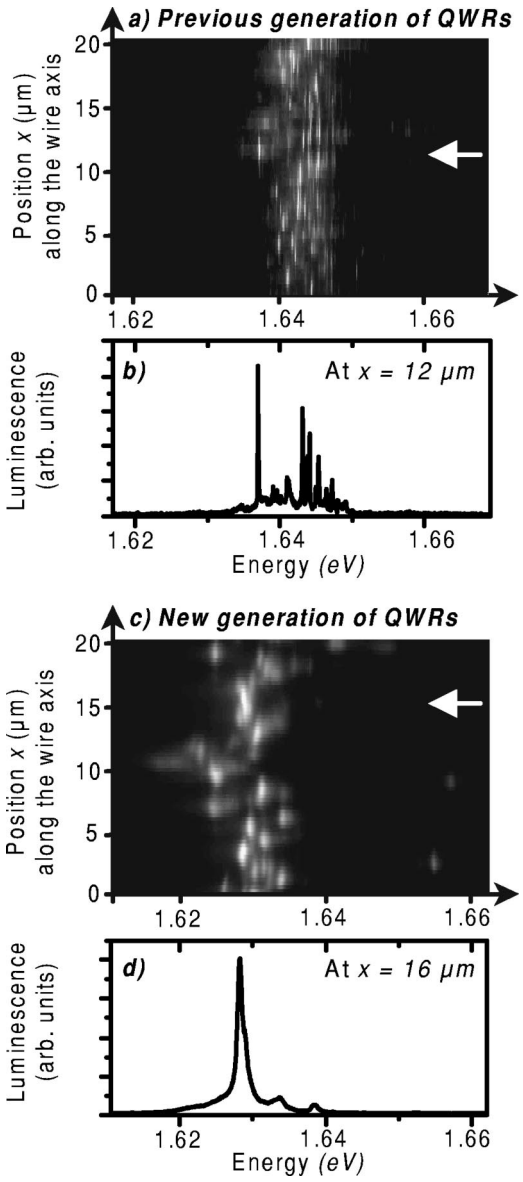

FIG. 1. Scanning optical images of a single wire of the previous (a) and the new (c) generation of QWR's. The μ-PL intensity is represented in gray levels. Typical μ-PL spectra, extracted from these images at the positions indicated by white arrows, are presented in (b) and (d).

These properties have been studied and compared more quantitatively through a statistical analysis of the images, which is described in detail in the Appendix. It allows us to define two mean properties of the localization sites in a given sample: the mean spectrum and the mean spatial distribution of its luminescence. They are presented in Fig. 2. In the spatial dimension [Fig. 2(a)], the mean distribution of the luminescence emitted by one site has a full width at half maximum (FWHM) of 0.8 μm for the previous generation, corresponding to the spatial resolution of the microscope, since the emitting sites are much smaller than the resolution and can be considered as point sources. The larger FWHM

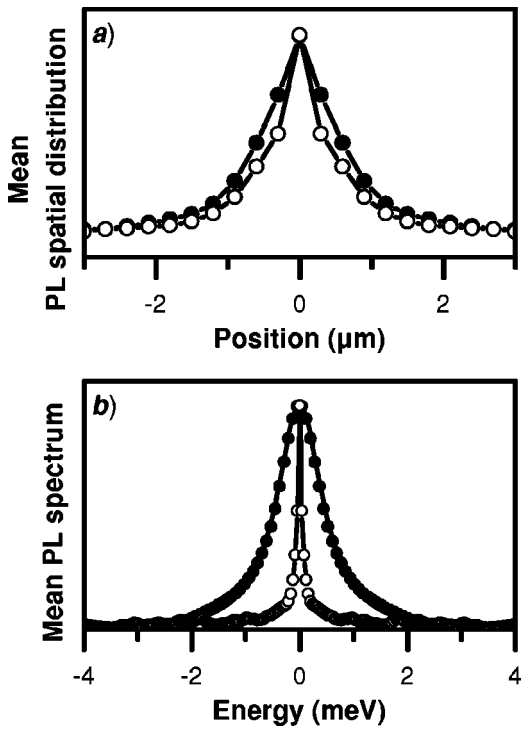

FIG. 2. Statistical mean properties of the localization sites in the previous (open dots) and new (plain dots) generations of QWR's: (a) mean spatial distribution of the emitted luminescence. (b) mean spectrum. The plain line is a fit by a Lorentzian line shape.

(1.2 μm) obtained for the new generation is due to the extension of the sites, which becomes comparable to the resolution of the microscope and can be estimated as 1.2 μm -0.8 μm$=0.4$ μm. In the spectral domain [Fig. 2(b)], the mean spectrum of the emitting sites for QWR's of the previous generation is very sharp as seen on individual spectra, whereas the one for the new generation of QWR's is perfectly fit by a 1-meV-broad Lorentzian line, which is even more clearly evidenced by the perfect triangular shape of its Fourier transform on a logaritmic scale over four decades, shown in Fig. 8(c). This broadening will be discussed in more detail in Sec. V.

The samples of the new generation are therefore of very high quality. For comparison, the longest reported localization length in V-groove QWR's as well as in any other kind of GaAs quantum wires is of the order of 600 nm and has been measured by SNOM only at one position of a given sample;[5] the typical extensions of the localization sites in the sample studied in this work were of 10–50 nm, and are comparable to those observed by our technique in the samples of the previous generation. In the new generation of QWR's, the large localization length of 400 nm is a mean property of the whole sample and obtained after a statistical analysis, the largest observed emitting sites being $2-3$ μm long. The consequences of this improvement on the optical properties of the excitons are discussed in the next section.

The enhancement of the localization length of excitons in the wires has been related to the structural properties of the samples. Indeed the localization of excitons is mainly due to the monolayer fluctuations of the interfaces of the wire, as

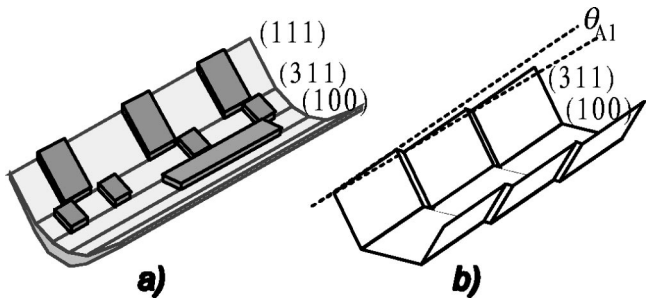

FIG. 3. (a) Monolayer fluctuations of the interfaces between the well and the barrier materials of the V-shaped wire; (b) monolayer steps induced by a misalignment of the V groove and the crystallographic direction $[1\bar{1}0]$.

schematically represented in Fig. 3(a). These interfaces have been identified on transmission electron micrographs (TEM) and are locally flat at the atomic level,[10] but they present monolayer steps which modify the confinement energy of the excitons in the wire. We calculated that the energy fluctuation associated to a monolayer step on the central facet (100) is about 9 meV, and the one for the lateral facets (311) and (111) is equal to 3 meV. These fluctuations can be directly identified on the images obtained on QWR's of the new generation [Fig. 1(c)]: the 3-meV ones are the most frequent (1 to 2 per μm) whereas the larger ones (about 10 meV, like at $x=10$ μm) are fewer (1 every 5 μm). These values correspond to the linear density of monolayer steps on the lateral and central facets, respectively, typically one step every 500 nm.

Three main changes in the fabrication of the samples have been developed in the past years. First of all, the chemical etching of the patterned sample allowed us to get smoother heterointerfaces between the well and the barrier materials, as shown by atomic force microscopy (AFM) images.[10] Second, the arsenic source for the epitaxy has been changed and tertiarybutylarsine (TBAs) is now used instead of the very toxic arsine (AsH_3). This leads to a strong diminution of the nonradiative recombination at room temperature, which is interpreted as the reduction of the impurity concentration in the sample.[11,13] The last and most crucial parameter is the misalignment angle θ_{Al} between the V groove drawn by lithography and the crystallographic direction $[1\bar{1}0]$ [Fig. 3(b)]. We performed scanning optical imaging spectroscopy on samples grown in the same conditions but presenting different misalignments. The statistical analysis revealed that the linear density of emitting sites decreases from 4 to 1 μm^{-1} as the angle θ_{Al} is decreased from 0.1° to less than 0.004° by improving the alignment procedure. This confirms that the localization length is governed in good samples by the distance between monolayer steps on the lateral interfaces of the V groove, i.e., by the alignment of the V on the crystallographic direction.

III. LOCALIZATION, EXCITONIC EIGENSTATES AND DENSITY OF STATES

The enhancement of the localization length in the wires implies not only a quantitative, but also a qualitative change

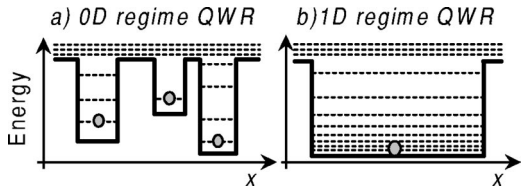

FIG. 4. Schematic representation of the eigenstates of the localization potential in the previous generation of QWR's, in the 0D regime ($V_{loc}=9$ meV, $L_{loc}\approx 30$ nm) (a), and in the new generation, in the 1D regime ($V_{loc}=9$ meV, $L_{loc}\approx 500$ nm) (b).

of their electronic properties. First of all, let us briefly consider the competition between the electron and hole localization and the Coulomb interaction. In both generations of QWR's, the amplitude of about 10 meV of the localization potential is smaller than the exciton binding energy, which is of the order of 20 meV, and the localization length scale is larger than the exciton Bohr radius $a_X=7$ nm.[14] The localization Hamiltonian can therefore be treated as a perturbation on the free rigid exciton model, and the localization potential felt by the excitons is simply the average over the wave function of the exciton relative motion (i.e., over a_X) of the potential felt by electrons and holes.

We should also compare the localization length L_{loc} of the excitons to their thermal de Broglie wavelength $\lambda_{Th}=\sqrt{2\pi\hbar^2/m_X k_B T}$, where the exciton mass $m_X\approx 0.18\ m_0$ is the sum of the electron and hole masses.[15] It is equal to about 50 nm at $T=10$ K in the wires we have studied. If $L_{loc}\gg\lambda_{Th}$, the energy difference between the eigenstates of the localization potential, typically $\hbar^2\pi^2/2m_X L_{loc}^2$, is much smaller than the thermal energy $k_B T$ and these eigenstates can be approximated by a 1D continuum of excitons. In the opposite case, when λ_{Th} is comparable to or larger than L_{loc}, only one or two localized states are populated at thermal equilibrium and the density of localized states is discrete. Since most of the microscopic properties of the excitons—relaxation, recombination—are determined by the local exciton density of states, the criterium $\lambda_{Th}\ll L_{loc}$ determines the one-dimensional character of the system. In the quantum wires of the previous generation, it is not fulfilled and the optical properties are those of a collection of quantum boxes, as our previous studies of the exciton relaxation, recombination[8] (cf. Sec. IV) and fine structure[9] have demonstrated; these wires are therefore said to be in the ''0D regime.'' On the contrary, in the new generation of QWR's, $\lambda_{Th}\ll L_{loc}$, so that each localizing site can be considered as a small portion of quantum wire with a continuum of 1D states; these sites are called ''islands'' in the following, in analogy with the situation in quantum wells, and the QWR's are said to be in the ''1D regime.'' The two regimes are schematically depicted in Fig. 4.

This interpretation is valid on a local point of view, as far as microscopic properties of the wires are concerned. On a macroscopic scale, the electronic properties are in both regimes inhomogeneously broadened of about 5–10 meV due to the variations of the confinement energy associated to monolayer fluctuations. This is different from the situation in quantum wells, where only one or two sharp peaks associated to two well thicknesses of N and $N+1$ monolayers are observed in the best samples.[16] In the case of QWR's, monolayer fluctuations on each of the heterointerfaces of the V give rise to a large number of possible configurations for the confinement, and therefore to an inhomogeneous broadening of the photoluminescence spectra.

It is here interesting to compare the different techniques used to study localization in QW's and QWR's, and to understand how they are adapted to specific localization regimes. In this paper we present two methods: the scanning imaging of the sample allows to directly measure the localization length in the 1D regime QWR's, when L_{loc} is comparable to the resolution of the microscope. But in the 0D regime QWR's L_{loc} is too small and only the linear density n of localizing sites can be obtained from the images, which gives an upper limit $L_{loc}<1/n$. In the 0D regime QWR's, we have shown in previous works[8] that the PL excitation spectra of each quantum box allow us to determine their extension from the energy separation between ground and excited states. But this is only valid if the quantum boxes are independent and if they contain two or more confined states, i.e., if roughly $V_{loc}>\hbar^2\pi^2/(2m_X L_{loc}^2)$. For smaller amplitude or typical length of the potential, the localized excitonic states extend over a few potential minima if $V_{loc}<\hbar^2\pi^2/(2m_X L_{loc}^2)$, and the eigenenergies are strongly spatially correlated. This is known as the level repulsion. Recently Idrissi *et al.* reported evidences for a level repulsion in QWR's very similar to our 0D regime QWR's.[17] In our statistical analysis, we were able to extract the same autocorrelation function $[R_c(E)]$ as they do, but we did not see any signature of this effect in our results. This can be explained by two practical reasons: (i) the cusp in the $R_c(E)$ which is characteristic of the level repulsion may be too small to be distinguished from the statistical noise in our case, even if we averaged over a 35-μm-long image; (ii) our spatial resolution is four times larger than the one of the SNOM experiment used in this work and is therefore much larger than the localization length, so that the spatial filtering of the correlations is less efficient. But it could also reflect that our 0D regime QWR's fulfill the condition $V_{loc}>\hbar^2\pi^2/(2m_X L_{loc}^2)$, so that the quantum boxes can be considered as isolated and no level repulsion exists if only the ground states emit luminescence. This is supported by our full understanding of the dynamics and spectroscopy of the excitons in 0D regime QWR's (Ref. 8) as those of isolated quantum boxes.

IV. RADIATIVE RECOMBINATION AND LOCALIZATION REGIME

The optical property which depends at the most on the density of states is the radiative lifetime τ_{rad}.[18–20] Its dependance on the temperature directly reflects the dimensionality of the exciton system: τ_{rad} scales as T for quantum wells, $\sqrt{T}$ for perfect quantum wires, and is independent of temperature for quantum boxes as soon as $k_B T$ is smaller than the energy separation between the two first states of the quantum box.

In 0D regime QWR's, the radiative lifetime has already been studied in μ-PL in previous works.[8] It is strongly de-

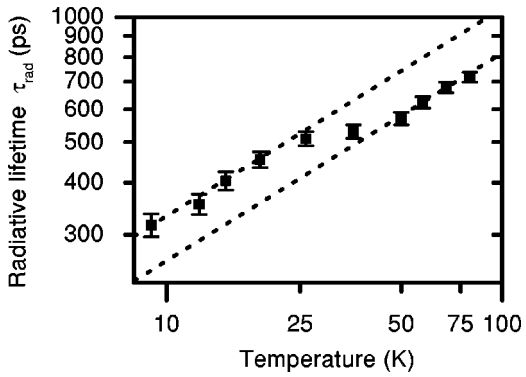

FIG. 5. Temperature dependence of the radiative lifetime of a single extended island in a 1D regime QWR. Two fits by a $\sqrt{T}$ dependence are presented by dotted lines (see text).

pendent on the quantum box under study and is in fact inversely proportional to the length of the quantum box. It is independent of temperature below 20 K. These results were interpreted in the following way: the typical energy separation between the quantum box states, of 2–5 meV, is larger than k_BT, so that at $T=10$ K, only the ground state of the quantum box is populated and τ_{rad} is independent of T. The oscillator strength of the ground state is proportional to the ratio of the coherence volume to the volume of the exciton relative motion wave function.[18,21] The latter one is independent of the localization length since $L_{loc} \gg a_X$, and the coherence volume is proportional to the length L_{loc} of the quantum box. So that the radiative lifetime at 10 K is inversely proportional to the length of the quantum box, as it has been measured experimentally.[8]

In 1D regime quantum wires, the radiative lifetime has been measured on several different wires and several samples, and is at 10 K independent of the island under consideration within 10%. The results obtained on one island as a function of temperature are presented in Fig. 5. The island chosen in the presented results is extended over 2 μm according to the scanning optical image. The measurements are performed in the low-density regime, and in average one exciton at the most is present in the excited island. The decay time of the PL is equal to the radiative lifetime since nonradiative recombination enters into play only above 200 K in these samples.[13] τ_{rad} follows a $\sqrt{T}$ scaling law below 30 K and above 50 K, which is characteristic of a 1D system. We do not observe any saturation of τ_{rad} at low temperature down to 8 K, which is the lowest temperature we can achieve in our μ-PL cryostat.

The $\sqrt{T}$ dependence of τ_{rad} can be briefly explained in the following way: if we consider free excitons, only those with a wave vector smaller than the one of light $k_\nu = 2\pi/\lambda$ can recombine radiatively, where λ is the wavelength of light in the material. The radiative exciton states form a band which spectral width is given by $\Delta_{rad} = \hbar^2 k_\nu^2 / 2m_X \approx 200$ μeV, and are assumed to have all the same recombination time τ^0_{rad}. At low density, the excitons in the band follow a Boltzmann distribution and the effective radiative lifetime of the wire is given by the thermal equilibrium between radiative and nonradiative states: if $\Delta_{rad} \ll k_BT$,[18,19]

$$\tau_{rad} = \tau^0_{rad} \sqrt{\frac{\pi\, k_BT}{4\Delta_{rad}}}. \quad (1)$$

The intrinsic recombination time deduced from the experimental results below 30 K is $\tau^0_{rad} = 170 \pm 20$ ps. It is comparable to the value of 150 ps theoretically predicted by Citrin in such wires[19]. We note that it is much larger than in QW's (a few 10 ps), as expected: for similar sizes, the 1D and 2D intrinsic lifetime should differ by a factor λ/a_X.[20] Moreover, the $\sqrt{T}$ dependence of τ_{rad} shows that the excitons are locally at thermal equilibrium at the bottom of the band in each island, and their density of states averaged over k_BT scales like $1/\sqrt{E-E_0}$.

The transition around 40 K is not fully understood at the moment, but two assumptions can be put forward: this temperature corresponds to the typical energy fluctuations along the wire axis (3 meV), so that the exciton density of states could be increased above 3 meV leading to a diminution of τ_{rad} above 40 K with respect to the situation in a single isolated island; the second possible hypothesis is that the coupling between excitons and acoustic phonons becomes strong above 50 K and could modify the exciton effective mass and/or their coherence time.[22]

Our results are comparable to those obtained by Akiyama *et al.*,[20] but they are more precise in the low-temperature range where localization effects influence the dependence of τ_{rad} on T. Moreover, they extend over a wider range of temperature and are not limited above 50 K by nonradiative recombination processes. The effect of localization in 0D regime QWR's has also been clearly evidenced by Oberli *et al.*, who observed and modeled the saturation of τ_{rad} below 20 K.[23]

V. RESIDUAL DISORDER IN 1D-REGIME QUANTUM WIRES

The μ-PL spectra of single islands present a broadening of about 1 meV which has to be explained. The individual spectra and even more clearly the mean spectrum obtained by the statistical analysis (Fig. 2) exhibit a perfectly Lorentzian line shape which is typical of an homogeneous broadening of the transition. However, the measured linewidth corresponds to a dephasing time T_2 for the excitons of the order of a picosecond. This dephasing time is too short to be associated to intrinsic dephasing mechanisms: we measured a recombination time of the order of 300 ps and we calculated that the interaction with acoustical phonons leads to a dephasing time of 10 ps at $T=10$ K for the excitons at the bottom of the band.[22]

We therefore have to consider other processes to explain this broadening. A static disorder, such as the alloy disorder in the barrier material or the atomic roughness of the interfaces, would lead to a Gaussian inhomogeneous broadening of the transition. But a dynamical disorder, like Coulomb collisions with impurities or charges could be involved and explain the fast dephasing of excitons. A signature of this disorder has been found in the μ-PL spectra under very weak

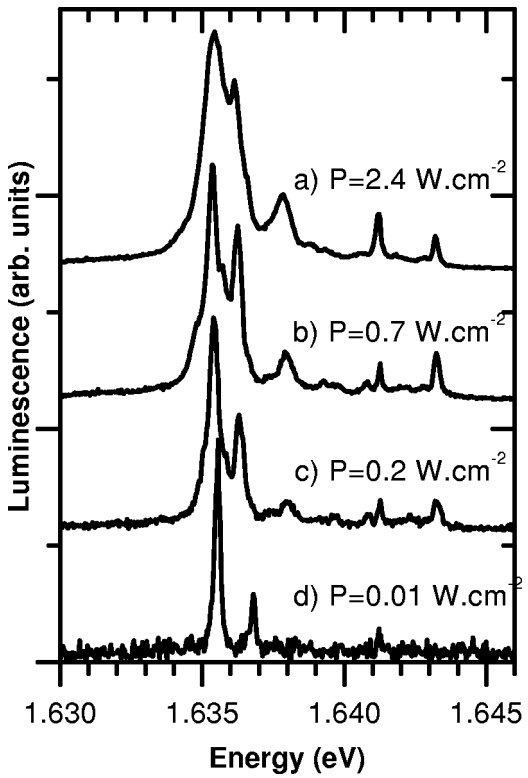

FIG. 6. PL spectrum of a single extended island in a 1D regime QWR at very low excitation power.

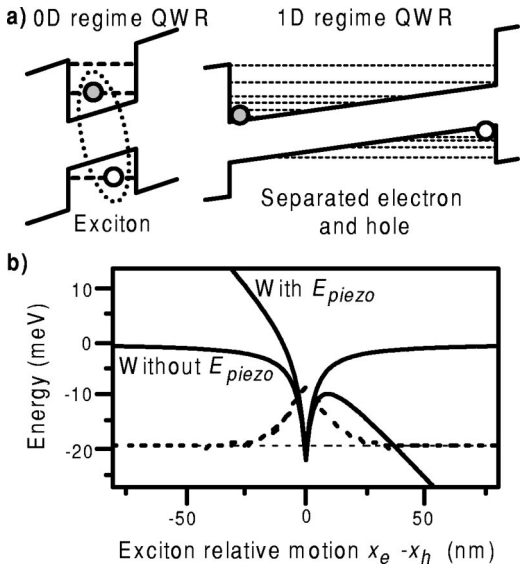

FIG. 7. (a) Effect of the piezoelectric field along the axis of the wire in both localization regimes. (b) In the case of 1D regime QWR's, the plain lines represent the potential felt by the relative motion of the electron-hole pair without the piezoelectric field (only Coulomb attraction) and with it (Coulomb + constant electric field), in the referential of the center of motion; the wave function of the unperturbed ground exciton state is also shown by dotted line.

excitation. Figure 6 presents the spectrum of a single island extended over 2 μm in a 1D regime QWR, as a function of the excitation power. We should underline that the excitation power P_0 necessary to create one exciton in the excitation spot every 300 ps (the radiative lifetime at $T=10$ K) is equal to 400 W cm^{-2}, as it has been measured in 0D and 1D regime QWR's by studying the formation of a biexciton.[22,24] It is 1000 times larger than the excitation power range presented in Fig. 6. We observe that the spectrum is composed of a main line, corresponding to the emission of the island, and four side peaks associated to neighboring islands present in the tails of the excitation spot. The main peak gets narrower as the excitation power is decreased, and it is not spectrally resolved at the lowest power—our resolution is 100 μeV in this experiment. This narrowing is therefore occuring as one exciton is created every 500 ns in the island, which is a crude estimation taking into account the power ratio between P_0 and the power range of the experiments presented in Fig. 6. The integrated intensity of the spectra is proportional to the excitation power, so that there is no new nonradiative recombination channel in this regime. Such line narrowing can only be explained if the electron and the hole are somehow spatially separated in the island since the recombination probability is proportional to the overlap of their wave functions.

This charge separation is attributed to the large piezoelectric field which exists along the axis of the wire as discussed in Ref. 25. The field is sufficient to separate electrons and holes only in 1D regime QWR's, in which the islands are large enough, whereas in 0D regime QWR's the exciton confined in a given quantum box is only deformed by the field. This is schematically depicted in Fig. 7(a). However, the piezoelectric field is not large enough to break an exciton if it is already formed: the bound electron-hole state still exists. As shown in Fig. 7(b), there are therefore two possible states: one bound exciton state centered on $x_e-x_h=0$, and one separated electron-hole pair state for large electron-hole separations ($x_e-x_h>50$ nm).

We can now explain the evolution of the spectrum with the excitation power: at the lowest power (0.01 W cm^{-2}), only one electron-hole pair is present in the island in a separated state. The transition between the separated electron-hole pair state and the bound exciton state is probably thermally activated and occurs within a few hundreds of ns. Then the exciton recombines, leading to a sharp PL peak. As the excitation power is increased, and during the linear regime until P_0 is reached, a few separated pairs accumulate in the island before they can form excitons, creating a background of free carriers that scatter the excitons, and leading to the broadening of the PL exciton line.

The homogeneous broadening of 1 meV of the μ-PL peaks in the linear regime (below P_0) is therefore a signature of a residual disorder, i.e., the Coulomb collisions between the excitons and separated carriers. These collisions occur on a timescale of 1 ps, much faster than the radiative lifetime of excitons, leading to a fast dephasing and a Lorentzian lineshape. The delocalized character of excitons in 1D regime QWR's makes them more sensitive to the piezoelectric field. This explains why the broadening was not observed in the spectra of quantum boxes in 0D regime QWR's in the same range of excitation power.

VI. CONCLUSION

By performing scanning optical imaging spectroscopy on different generations of QWR's, we studied the disorder and especially the localization length of the excitons. In the best samples, excitons are delocalized over 400 nm in average and up to 2–3 μm in the most extended islands. Indeed QWR's exhibit a localization length much larger than the thermal de Broglie wavelength of the excitons, which therefore form in each island a 1D quasicontinuum. On the opposite, in previous samples, the localization length is smaller than the de Broglie wavelength and the optical properties of the QWR's are those of a 0D system, i.e., a collection of quantum boxes. The 1D character of the local density of states in the best samples is evidenced by measuring the temperature dependence of the radiative lifetime: it follows a $\sqrt{T}$ scaling law down to the lowest achieved temperature (8 K), whereas a saturation below 20 K has been observed in previous works on 0D regime QWR's. Finally we show that the excitons are more sensitive to the residual disorder in the structure as they get delocalized, and the presence of photocreated charges separated by the built-in piezoelectric field leads to a homogeneous broadening of the transitions in μ-PL spectra.

APPENDIX STATISTICAL ANALYSIS OF THE IMAGES

The scanning images of QWR's provide us with an intuitive representation of the excitonic states along the wire, but they also contain more quantitative informations. It is, for example, very useful to obtain the spatial and spectral shape of the bright spots of the image, i.e., the spatial distribution and the spectrum of the localizing sites. However this cannot be done in a proper way by extracting the cross sections of one given bright spot because they all slightly overlap, as can be seen in Fig. 1. Moreover, such cross sections are specific to the localizing site considered and are not representative of all of them. We therefore analyzed the images by autocorrelation techniques, and calculated the mean spatial distribution and the mean spectrum of the localizing sites.

In order to present the different calculated correlations, we will suppose for simplicity that an image is composed of N spots with identical shapes but different amplitudes A_n, at an energy E_n and a position x_n. The μ-PL signal $F(E,x)$ at the position x and the energy E can be written

$$F(E,x)=\sum_n A_n u_E(E-E_n)\times u_x(x-x_n)$$
$$=[u_E(E)\times u_x(x)]\otimes D(E,x), \qquad \text{(A1)}$$

where u_E and u_x are the spectral and spatial shapes of the spots, and $D(E,x)=\Sigma_n A_n \delta(E-E_n)\,\delta(x-x_n)$ is the distribution of the spectral and spatial positions of the spots. Their Fourier transforms are noted $\tilde{u}_E(s)$, $\tilde{u}_x(k)$, and $\tilde{D}(s,k)$, respectively. Those three functions can be obtained by calculating the autoconvolutions of the image F. We will here focus on the spectral analysis, and the same study can be done in the spatial dimension.

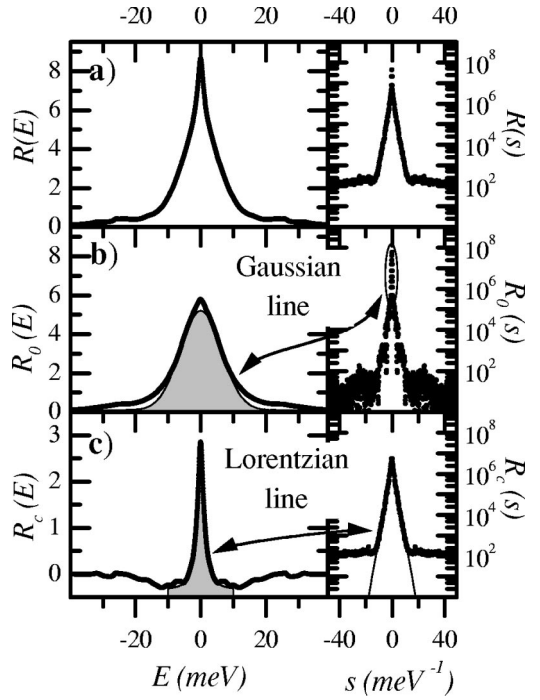

FIG. 8. (a) Spectral autoconvolution $R(E)$, (b) its spatially uncorrelated component $R_0(E)$, and (c) the autocorrelation $R_c(E)=R(E)-R_0(E)$, in the case of the image of Fig. 1(c) of a QWR of the new generation. The fitted line shapes (b) and (c) are presented in filled areas.

The spectral autoconvolution is defined as

$$R(E)=\langle\langle F(E',x)F(E-E',x)\rangle_{E'}\rangle_x, \qquad \text{(A2)}$$

where $\langle\rangle_\alpha$ denotes the average over the parameter α. It is the spatial average of the autoconvolution calculated at each position. It is represented in Fig. 8(a) with its Fourier transform $\tilde{R}(s)=|\tilde{F}(s,k=0)|^2$, for the image [Fig. 1(c)] of a QWR of the new generation. It is the sum of two terms: a spatially uncorrelated part $R_0(E)$ and a correlated one $R_c(E)$.

The uncorrelated autoconvolution [Fig. 8(b)] is equal to

$$R_0(E)=\langle\langle F(E',x)\rangle_x\langle F(E-E',x)\rangle_x\rangle_{E'}. \qquad \text{(A3)}$$

Its Fourier transform writes $\tilde{R}_0(s)=\langle|\tilde{F}(s,k)|^2\rangle_k$. For a sufficiently large image ($N\to\infty$), it tends to the autoconvolution of the macroluminescence spectrum $\langle D(E,x)\rangle_x=(1/N)\Sigma_n A_n\delta(E-E_n)$. Its linewidth of 12 meV corresponds to the inhomogeneous broadening of the PL spectrum multiplied by $\sqrt{2}$, as expected for a Gaussian shape.

The correlated part of $R(E)$, called the autocorrelation [Fig. 8(c)], is obtained as

$$R_c(E)=R(E)-R_0(E). \qquad \text{(A4)}$$

In the limit of large images and if the energy E_n of the spots are spatially uncorrelated, it tends to the autoconvolution of the spectral shape $u_E(E)$ of the spots. In the case of the image in Fig. 1(c), the auto-correlation is mainly composed of a 2.2-meV-broad Lorentzian line corresponding to the au-

toconvolution of u_E and a few side peaks at ± 9 meV, ± 12 meV, ..., which reflect the correlations between the energies of neighboring islands, i.e., the energy fluctuations associated to monolayer fluctuations.

In order to evaluate $u_E(E)$, we calculated the "mean" spectrum $f_c(E)$ of the islands, represented in Fig. 2, as the inverse Fourier transform of $\tilde{f}_c(s) = \sqrt{|\tilde{R}_c(s)|}$. It is correct if we suppose that u_E is an even function of E, so that $\tilde{f}_c(s)$ is real. In the case considered in Fig. 8(c), the Lorentzian character of the mean spectrum is even clearer on the Fourier transform $\tilde{R}_c(s)$, which is triangular over four decades in a logaritmic scale.

The same analysis can be reproduced in the spatial dimension and provides us with the mean spatial distribution of the luminescence emitted by the islands.

*Also at Département de Physique, Ecole Polytechnique Fédérale de Lausanne, Switzerland; electronic address: guillet@gps.jussieu.fr

†Also at Université Evry-Val d'Essonne, France.

‡Also at Department of Electrical Engineering, Yale University, New Haven, CT.

[1] G. Bastard, C. Delalande, M.H. Meynadier, P.M. Frijlink, and M. Voos, Phys. Rev. B **29**, 7042 (1984).

[2] F. Yang, M. Wilkinson, E.J. Austin, and K.P. O'Donnell, Phys. Rev. Lett. **70**, 323 (1993).

[3] J. Bellessa, V. Voliotis, R. Grousson, X.L. Wang, M. Ogura, and H. Matsuhata, Appl. Phys. Lett. **71**, 2481 (1997).

[4] F. Intonti, V. Emiliani, C. Lienau, T. Elsaesser, R. Nötzel, and K.H. Ploog, Phys. Rev. B **63**, 075313 (2001).

[5] A. Crottini, J.L. Staehli, B. Deveaud, X.L. Wang, and M. Ogura, Phys. Rev. B **63**, 121313 (2001).

[6] R. Zimmermann and E. Runge, Phys. Status Solidi A **164**, 511 (1997); Phys. Status Solidi B **206**, 167 (1998).

[7] Q. Wu, R.D. Grober, D. Gammon, and D.S. Katzer, Phys. Rev. B **62**, 13 022 (2000).

[8] J. Bellessa, V. Voliotis, R. Grousson, X.L. Wang, M. Ogura, and H. Matsuhata, Phys. Rev. B **58**, 9933 (1998).

[9] T. Guillet, V. Voliotis, R. Grousson, R. Ferreira, X.L. Wang, and M. Ogura, Physica E (Amsterdam) **9**, 686 (2001).

[10] X.L. Wang, V. Voliotis, R. Grousson, and M. Ogura, J. Cryst. Growth **213**, 19 (2000).

[11] X.L. Wang and M. Ogura, J. Cryst. Growth **221**, 556 (2000).

[12] X.L. Wang, M. Ogura, and H. Matsuhata, Appl. Phys. Lett. **67**, 804 (1995); J. Cryst. Growth **195**, 586 (1998).

[13] X.Q. Liu, X.L. Wang, and M. Ogura, Appl. Phys. Lett. **79**, 1622 (2001).

[14] M. Combescot and T. Guillet, Eur. Phys. J. B (to be published).

[15] We take $m_e = 0.067\ m_0$ for the electron mass and $m_h = 0.11\ m_0$ for the heavy hole mass along the wire axis x, expressed in terms of the bare electron mass m_0.

[16] D. Deveaud, T.C. Damen, and J. Shah, Appl. Phys. Lett. **51**, 828 (1987).

[17] A. Crottini, R. Idrissi-Kaitouni, J.L. Staehli, B. Deveaud, X.L. Wang, and M. Ogura, Phys. Status Solidi A **190**, 631 (2002).

[18] J. Feldmann, G. Peter, E.O. Göbel, P. Dawson, K. Moore, C. Foxon, and R.J. Elliott, Phys. Rev. Lett. **59**, 2337 (1987).

[19] D.S. Citrin, Phys. Rev. Lett. **69**, 3393 (1992).

[20] H. Akiyama, S. Koshiba, T. Someya, K. Wada, H. Noge, Y. Nakamura, T. Inoshita, A. Shimizu, and H. Sakaki, Phys. Rev. Lett. **72**, 924 (1994).

[21] E.T. Rashba and G.E. Gurgenishvili, Fiz. Tverd. Tela (Leningrad) **4**, 759 (1962) [Sov. Phys. Solid State **4**, 759 (1962)].

[22] T. Guillet, Ph.D. thesis, Université Pierre et Marie Curie, Paris, 2002.

[23] D.Y. Oberli, M.A. Dupertuis, F. Reinhardt, and E. Kapon, Phys. Rev. B **59**, 2910 (1999).

[24] T. Guillet, R. Grousson, V. Voliotis, M. Menant, X.L. Wang, and M. Ogura, Phys. Rev. B **67**, 235324 (2003).

[25] X.Q. Liu, X.L. Wang, M. Ogura, T. Guillet, V. Voliotis, and R. Grousson, Appl. Phys. Lett. **80**, 1894 (2002).